國立中央大學
National Central University

3D EFFECTS OF PERMEABILITY AND STRENGTH ANISOTROPY ON THE STABILITY OF WEAKLY CEMENTED ROCK SLOPES SUBJECTED TO RAINFALL INFILTRATION

AUTHORS: PO-TSUN YEH, KEVIN ZEH-ZON LEE, KUANG-TSUNG CHANG

AFFILIATIONS: NATIONAL CHUNG HSING UNIVERSITY, TAIWAN; U.S. BUREAU OF RECLAMATION, DENVER, USA

PRESENTER: CHENG-KUANG CHANG

ADVISOR: PROF. JIA-JYUN DONG

DATE: 2024/11/08

MOTIVATION FOR CHOOSING THIS TOPIC BACKGROUND

- I COMPLETED MY UNDERGRADUATE STUDIES IN CIVIL ENGINEERING, EARNED A MASTER'S DEGREE IN SOIL AND WATER CONSERVATION, AND AM CURRENTLY PURSUING A PH.D. IN APPLIED GEOLOGY.
- I NOW RUN AN ENGINEERING CONSULTING COMPANY, FOCUSING PRIMARILY ON HILLSIDE DEVELOPMENT PROJECTS, WHERE SLOPE STABILITY ANALYSIS IS FREQUENTLY REQUIRED.

RESEARCH MOTIVATION:

- ALTHOUGH I ENCOUNTER SLOPE STABILITY ISSUES REGULARLY IN MY WORK, I HAVE NOT YET EXPLORED THE IMPACT OF RAINFALL INFILTRATION AND STRENGTH ANISOTROPY IN-DEPTH.
- THIS STUDY OFFERS AN OPPORTUNITY TO DELVE INTO THESE CRITICAL ASPECTS, WITH THE AIM OF ENHANCING THE SCIENTIFIC FOUNDATION FOR FUTURE PRACTICAL APPLICATIONS.

INTRODUCTION

BACKGROUND:

- WEAKLY CEMENTED ROCKS IN SEDIMENTARY ENVIRONMENTS EXHIBIT DISTINCT PERMEABILITY AND STRENGTH ANISOTROPY.
- RAINFALL INFILTRATION SIGNIFICANTLY IMPACTS SLOPE STABILITY, ESPECIALLY UNDER VARYING ORIENTATIONS OF BEDDING PLANES.

RESEARCH AIM:

- TO ASSESS THE EFFECT OF PERMEABILITY AND STRENGTH ANISOTROPY ON SLOPE STABILITY USING 3D FINITE ELEMENT MODELING.

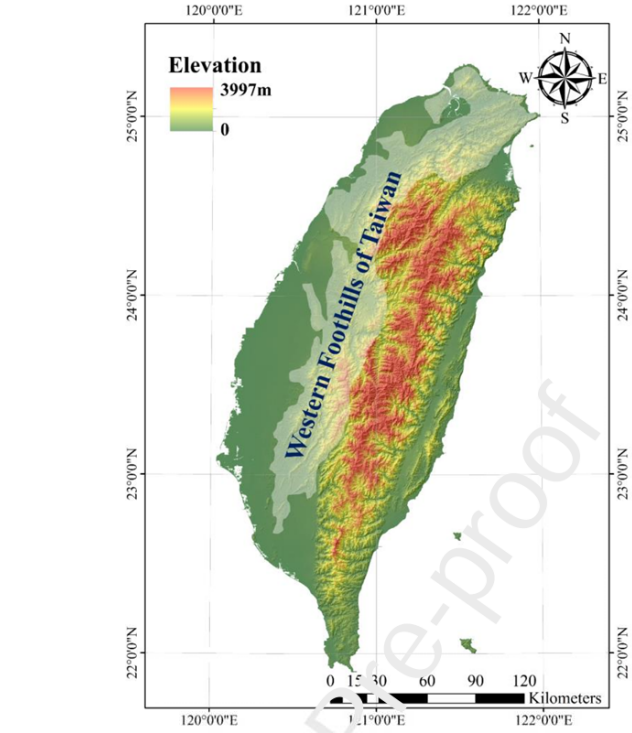

(a)

(b)

Fig. 1. (a) Location of the Western Foothills of Taiwan including weakly cemented sedimentary rocks and (b) weakly cemented thin alternating beds of shale and sandstone.

PROBLEM STATEMENT

CHALLENGES IN SLOPE STABILITY:

- INTERACTION BETWEEN RAINFALL INFILTRATION AND ANISOTROPIC GEOLOGICAL STRUCTURES.
- COMPLEXITY OF MODELING ANISOTROPY IN BOTH PERMEABILITY AND STRENGTH IN 3D SIMULATIONS.

HYPOTHESIS:

- THE ORIENTATION AND ANGLE OF BEDDING PLANES UNDER RAINFALL CONDITIONS SIGNIFICANTLY AFFECT SLOPE STABILITY.

METHODOLOGY – 3D MODELING APPROACH

SOFTWARE USED:

- FEMWATER FOR GROUNDWATER FLOW SIMULATIONS.
- PLAXIS 3D FOR STABILITY ANALYSIS.

MODEL PARAMETERS:

- DIFFERENT BEDDING PLANE ANGLES (E.G., 21.5° AND 60°) TO SIMULATE GENTLY AND STEEPLY DIPPING SLOPES.

BOUNDARY CONDITIONS:

- CONSTANT HEADS ON SLOPE SIDES AND A RAINFALL PATTERN MODELED AFTER TYPHOON MORAKOT.

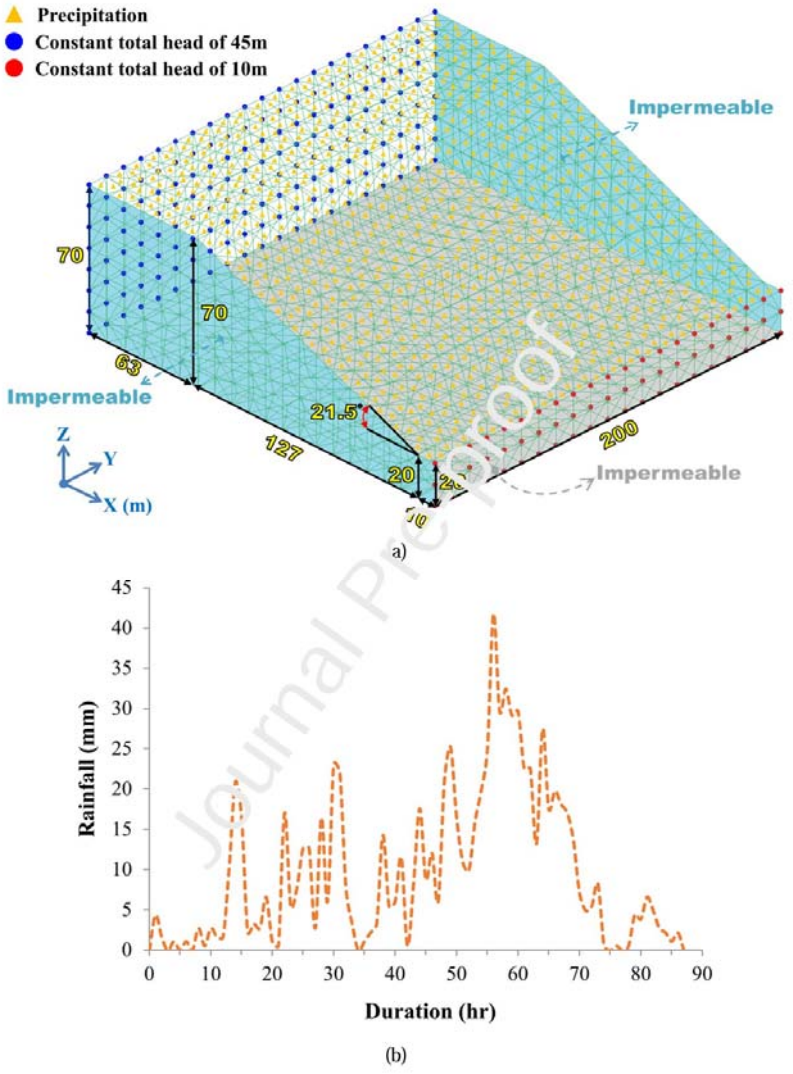

Fig. 2. The numerical model: (a) configuration and hydraulic boundary condition and (b) precipitation monitored at Lushan station during typhoon Morakot in 2009.

Table 1. Parameters used in the FEMWATER model.

Porosity	0.3
Compressibility of geo-material (Pa^{-1})	1.3×10^{-9}
Viscosity of water ($Pa \cdot s$)	8.9×10^{-4}
Compressibility of water (Pa^{-1})	4.7×10^{-10}
Permeability coefficient parallel to bedding planes (cm/s)	6×10^{-6}
Permeability coefficient perpendicular to bedding planes (cm/s)	6×10^{-7}

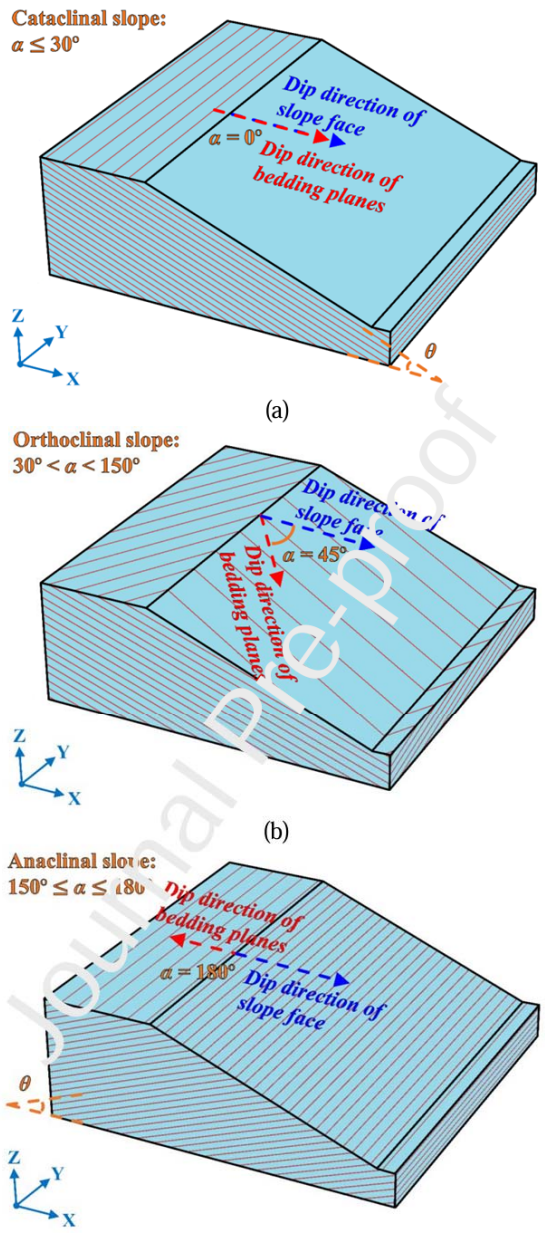

Fig. 3. Definition of α (the angle between the dip directions of the bedding planes and of the slope face) and θ (the dip angle of the bedding planes) as well as classification of bedding plane-slope relationships: (a) cataclinal (b) orthoclinal and (c) anaclinal slopes.

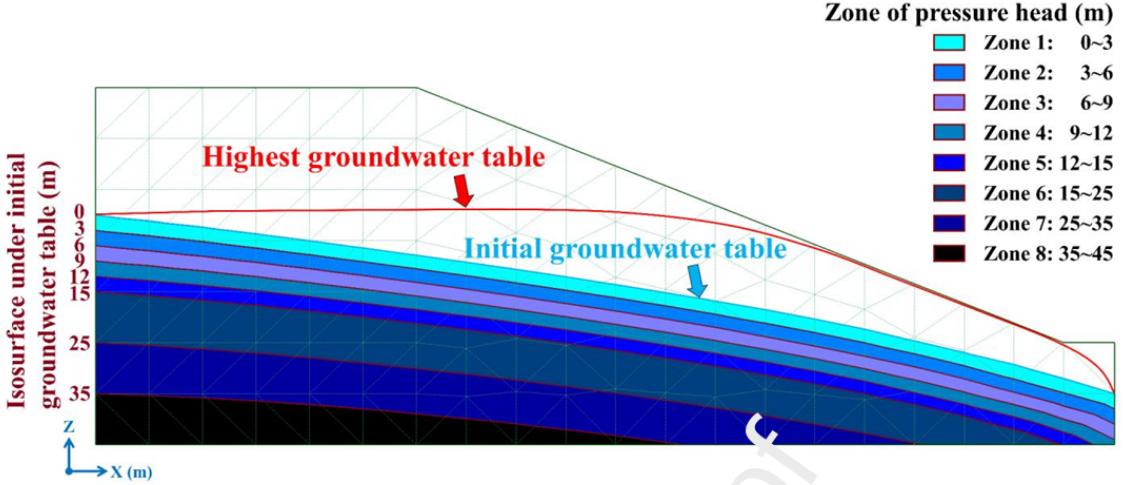

Fig. 4. Zones in a slope separated by isosurfaces below the initial groundwater table.

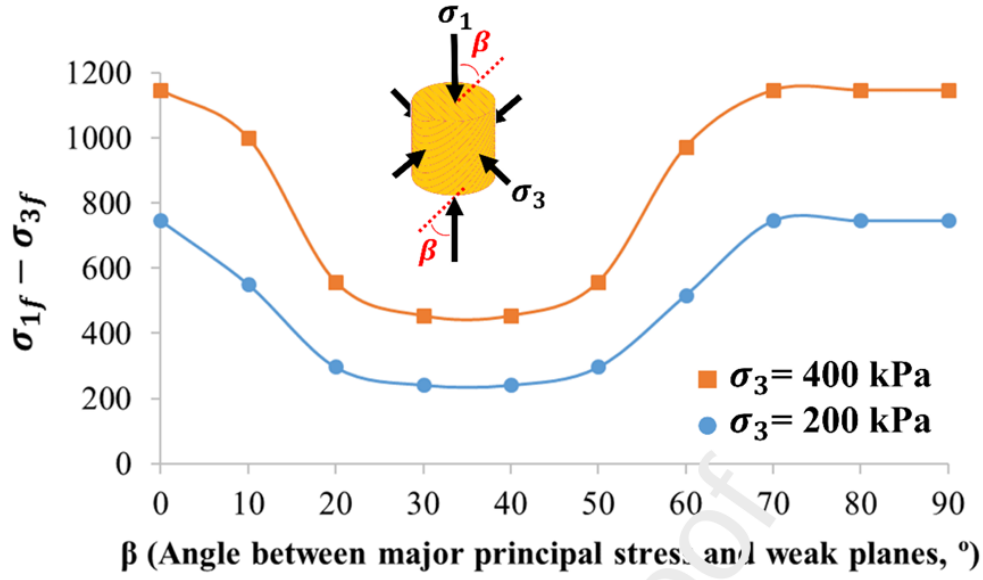

Fig. 5. Strength anisotropy in numerical triaxial compression.

METHODOLOGY – PERMEABILITY AND STRENGTH ANISOTROPY

PERMEABILITY ANISOTROPY:

- DEFINED AS THE RATIO OF PERMEABILITY PARALLEL VS. PERPENDICULAR TO BEDDING PLANES.
- PARALLEL PERMEABILITY: 6 X 10^{-6} CM/S; PERPENDICULAR: 6 X 10^{-7} CM/S.

STRENGTH ANISOTROPY:

- COHESION AND FRICTION ANGLE DIFFER FOR WEAK PLANES AND ROCK MATRIX.
- ROCK COHESION: 100 KPA, WEAK PLANE COHESION: 10 KPA.

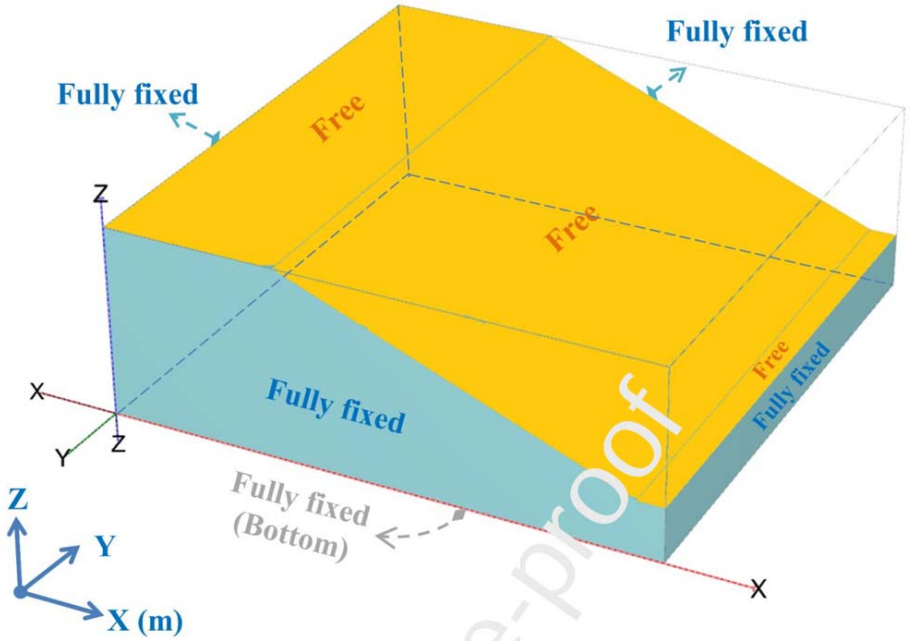

Fig. 6. The deformation boundary condition in the numerical model.

Table 2. Parameters used in the PLAXIS model.

γ_{unsat} (kN/m^3)	20
γ_{sat} (kN/m^3)	23
Shear modulus (kPa)	1.9×10^6
Poisson's ratio	0.3
Cohesion of weakly cemented rock (kPa)	100
Friction angle of weakly cemented rock (°)	30
Cohesion on weak plane (kPa)	10
Friction angle on weak plane (°)	20

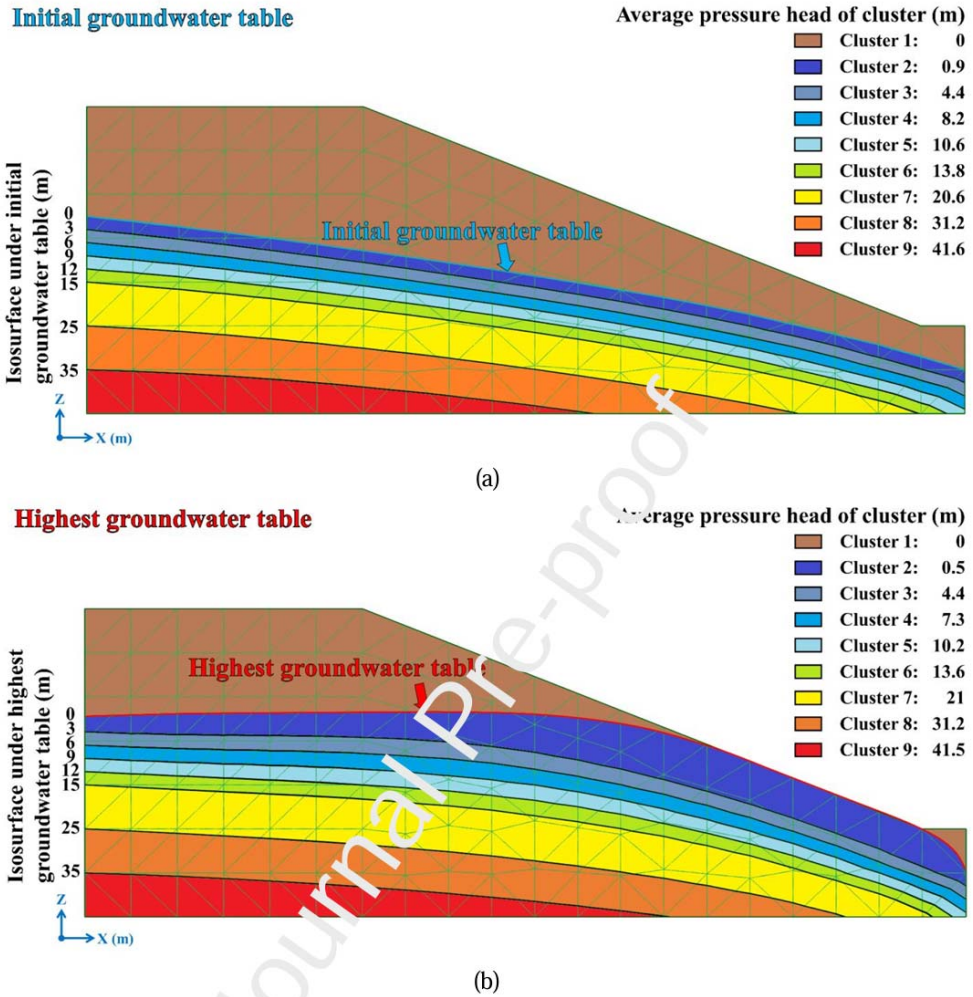

Fig. 7. Clusters in a slope showing different average pressure heads at conditions with: (a) the initial groundwater table and (b) the highest groundwater table.

METHODOLOGY – SIMULATION PROCESS

STEPS:

- 1. INITIAL CONDITION: SET INITIAL GROUNDWATER TABLE FOR THE SLOPE.
- 2. RAINFALL SIMULATION: APPLY 851 MM RAINFALL, PEAKING AT 42 MM/HR.
- 3. PRESSURE CALCULATION: EVALUATE PORE PRESSURE AND GROUNDWATER TABLE RISE.
- 4. STABILITY ANALYSIS: CALCULATE FACTOR OF SAFETY (FOS) PRE- AND POST-RAINFALL.

RESULTS – GROUNDWATER TABLE RISE

OBSERVATION:

- SLOPES WITH STEEPER BEDDING PLANES REACH PEAK GROUNDWATER LEVELS MORE QUICKLY.
- GRAPH: AVERAGE GROUNDWATER TABLE HEIGHT VS. TIME FOR VARIOUS SLOPE ORIENTATIONS.
- EXPLANATION: ANISOTROPIC PERMEABILITY ALLOWS FASTER UPWARD FLOW ALONG STEEPER PLANES.

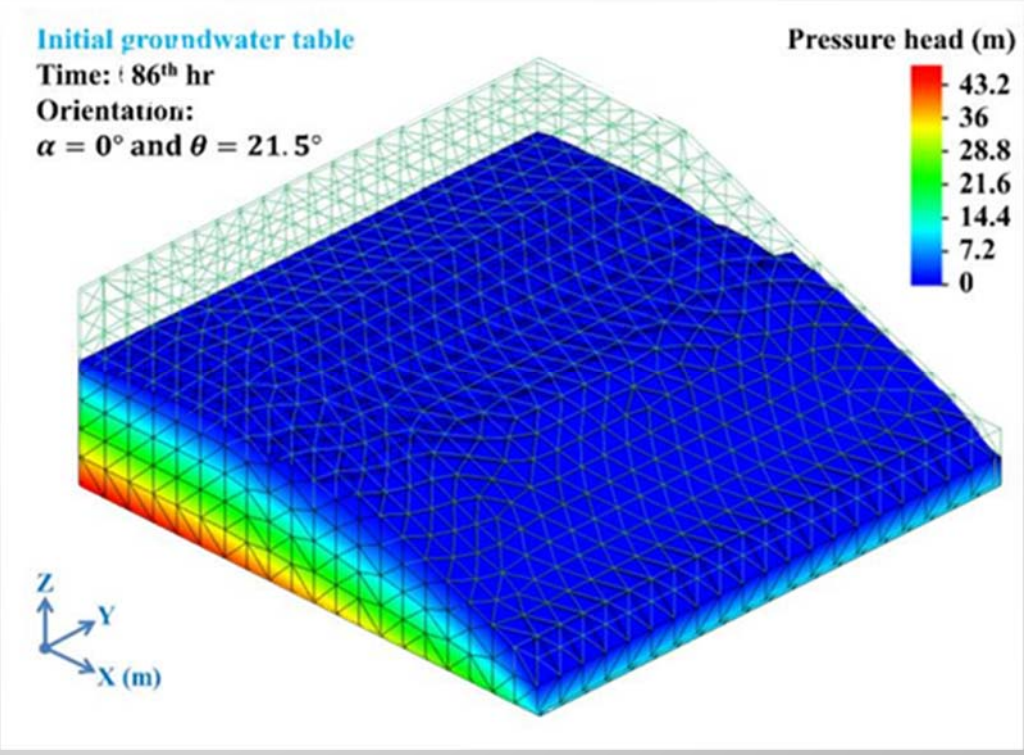

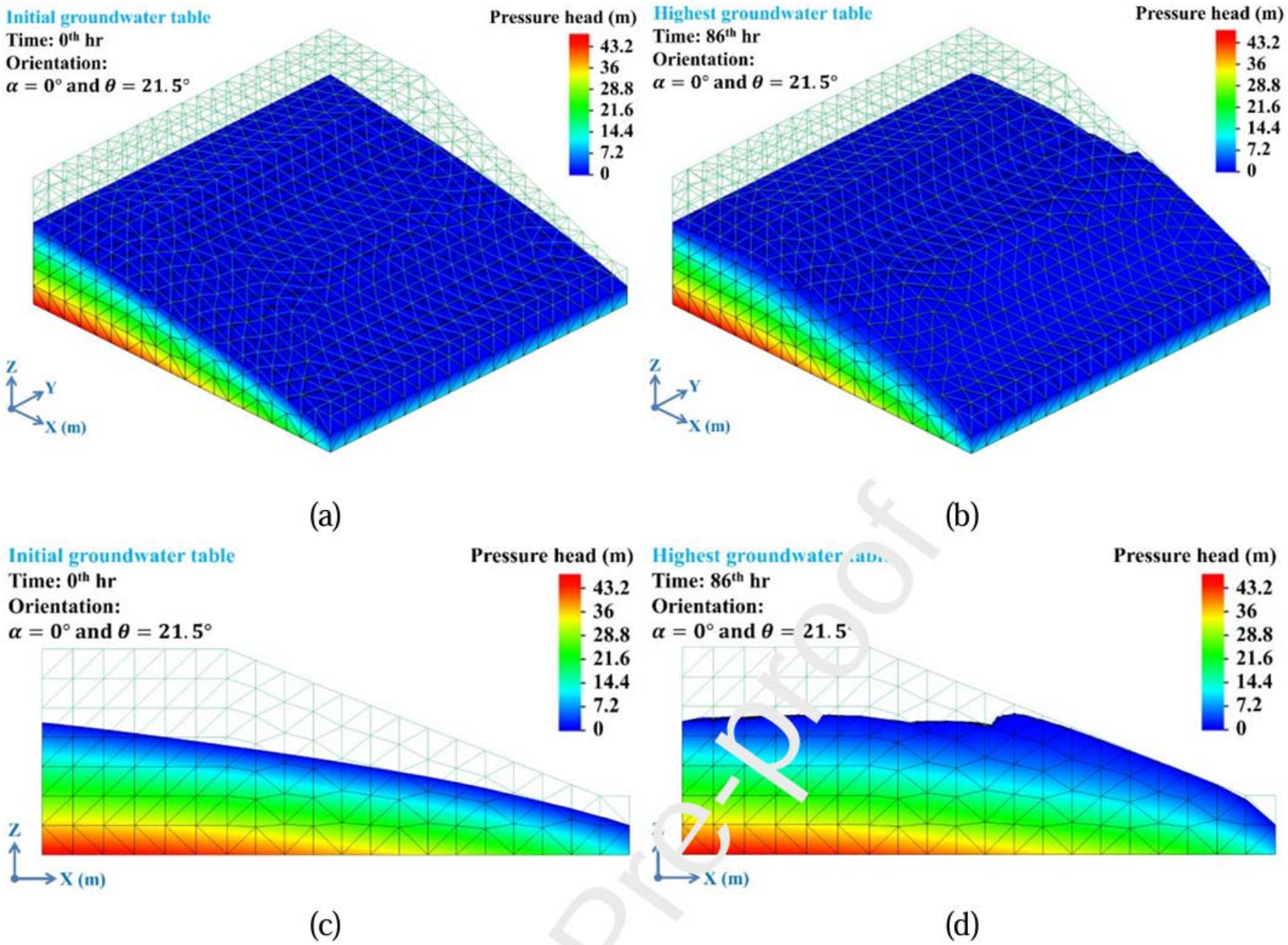

Fig. 8. Pressure head distributions under the initial and highest groundwater tables in the slope: (a) (b) oblique view and (c) (d) central longitudinal sections.

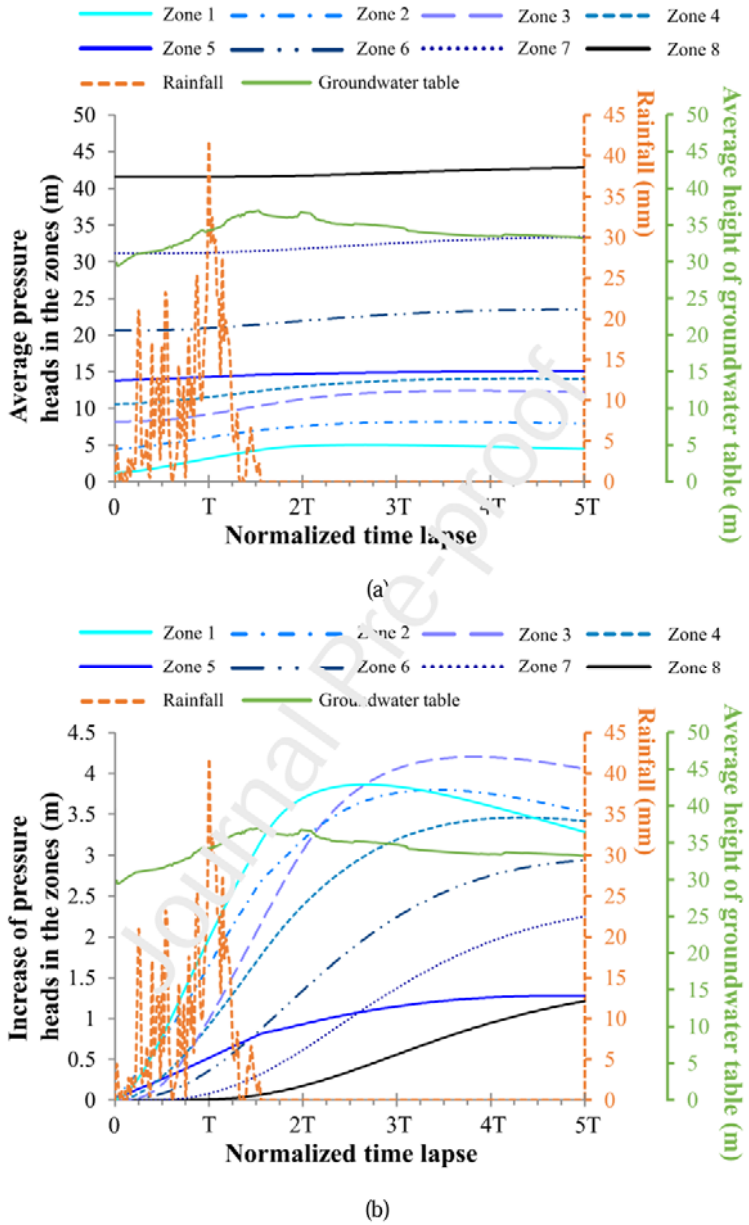

Fig. 9. Pressure heads and the average groundwater table in the slope ($\alpha = 0°$, $\theta = 21.5°$) during and after rainfall (T= 56 hrs): (a) pressure heads and (b) increase of pressure heads.

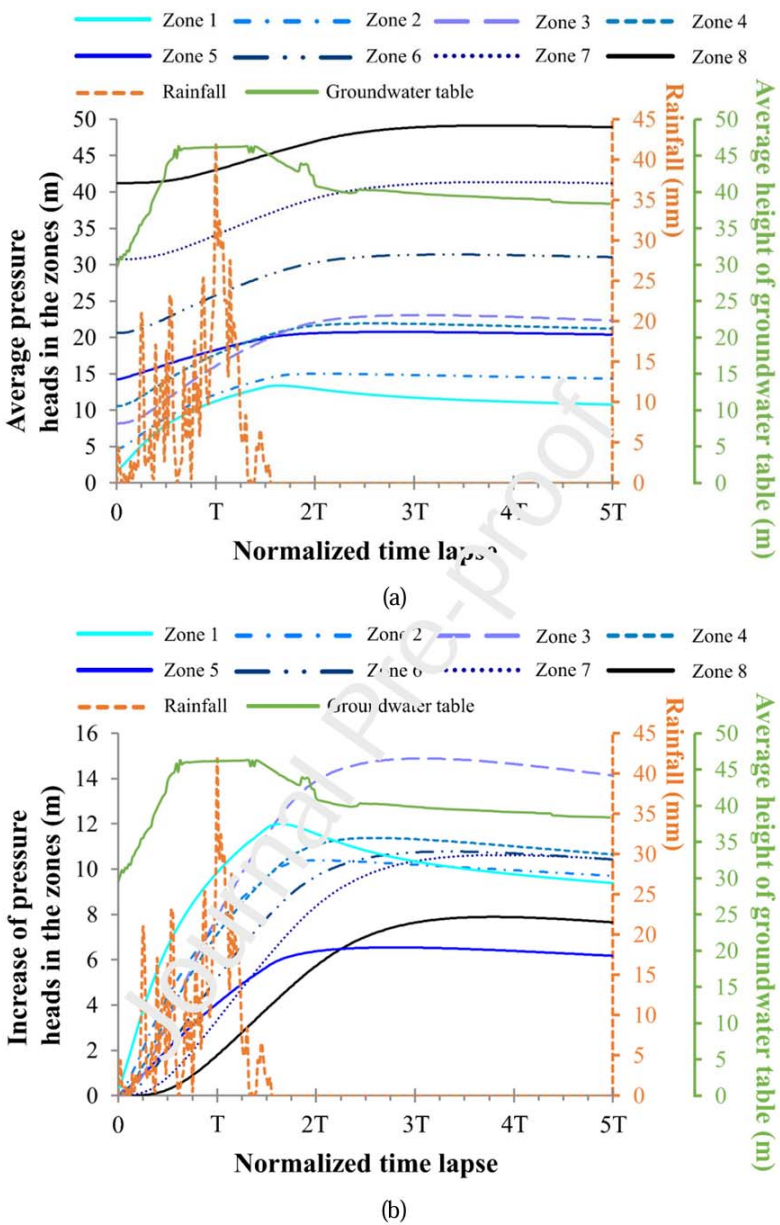

Fig. 10. Pressure heads and the average groundwater table in the slope ($\alpha = 0°$, $\theta = 60°$) during and after rainfall (T= 56 hrs): (a) pressure heads and (b) increase of pressure heads.

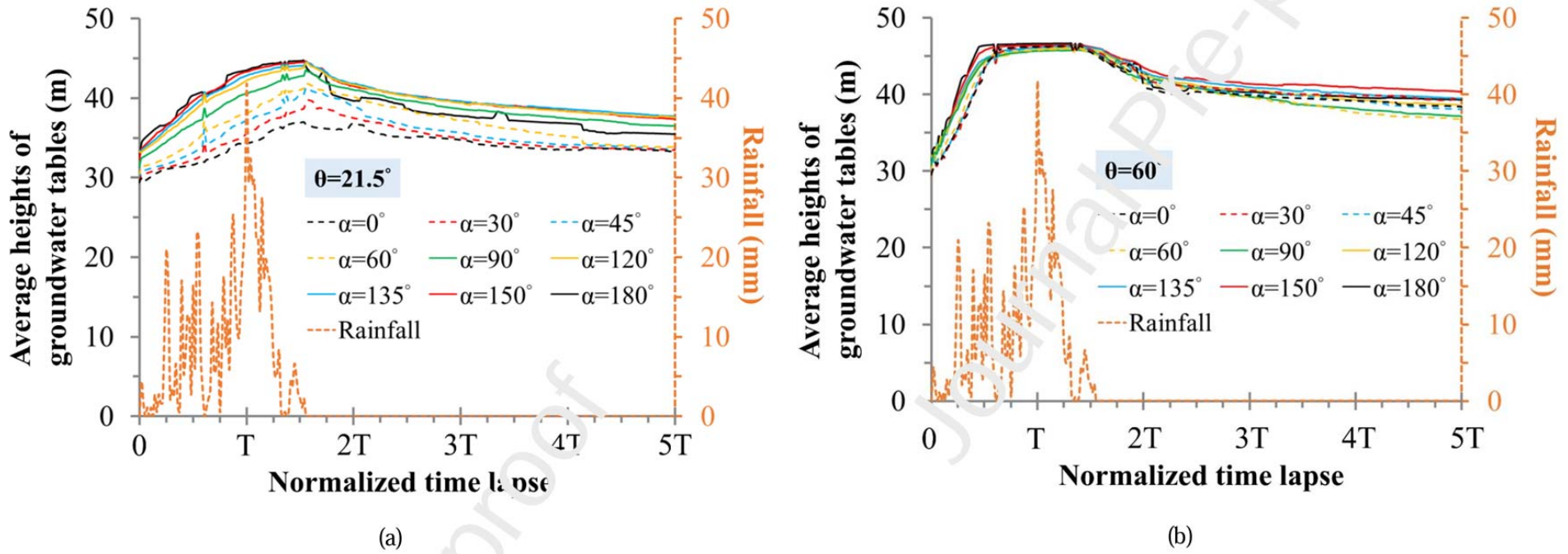

Fig. 11. Average heights of groundwater tables during and after rainfall for the slopes with various dip directions of bedding planes (T= 56 hrs): (a) dip angle of bedding planes = 21.5° and (b) dip angle of bedding planes = 60°.

RESULTS – PORE PRESSURE DISTRIBUTION

COMPARISON:

- HIGHER PORE PRESSURES OBSERVED IN SLOPES WITH STEEPLY DIPPING BEDDING PLANES.
- IMAGE: PRESSURE HEAD DISTRIBUTION UNDER INITIAL AND MAXIMUM GROUNDWATER LEVELS.
- KEY POINT: STEEP BEDDING PLANES ENHANCE PORE PRESSURE INCREASE AND ACCELERATE INSTABILITY.

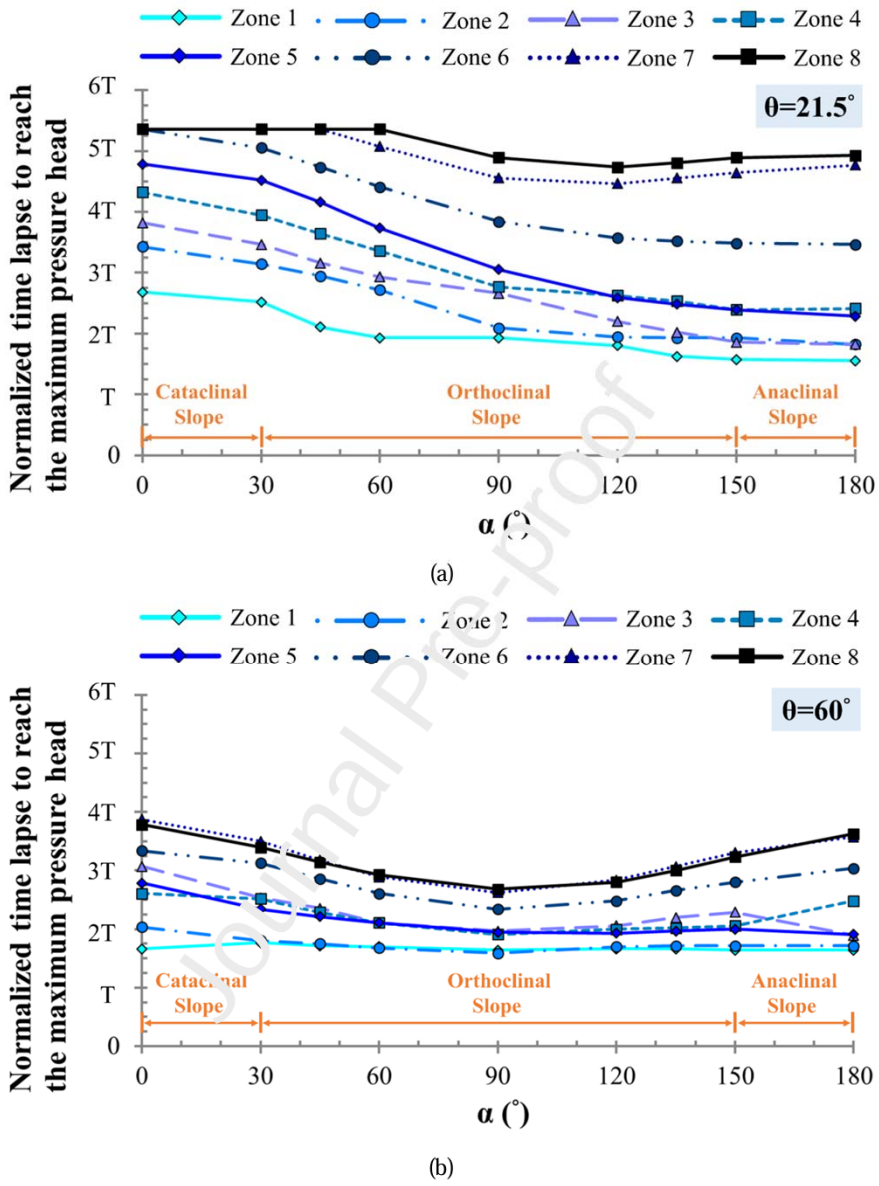

Fig. 12. Normalized time lapse to reach the maximum pressure heads in the zones considering various dip directions of bedding planes (T= 56 hrs): (a) dip angle of bedding planes = 21.5° and (b) dip angle of bedding planes = 60°.

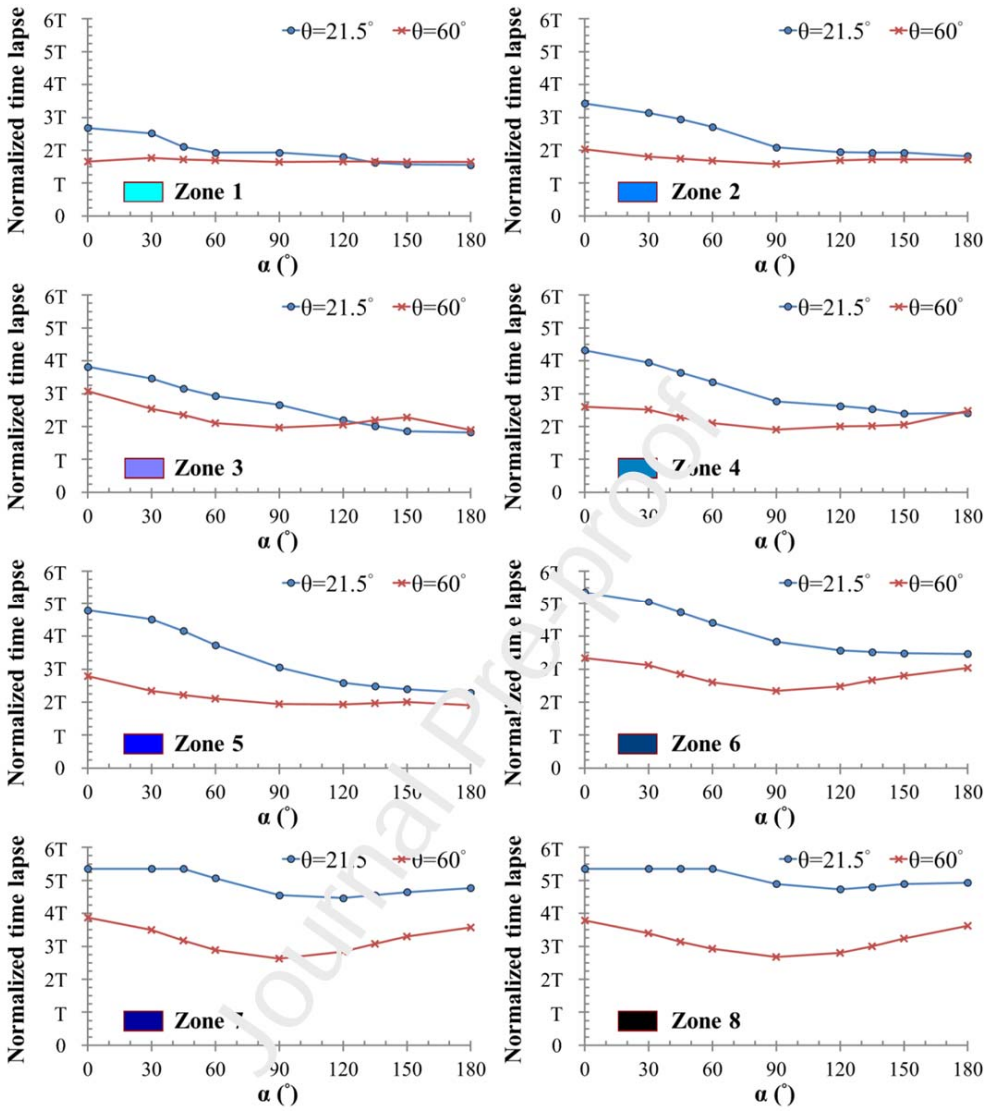

Fig. 13. Normalized time lapse to reach the maximum pressure head in each zone in comparison with the dip angles of bedding planes of 21.5° and 60° (T= 56 hrs).

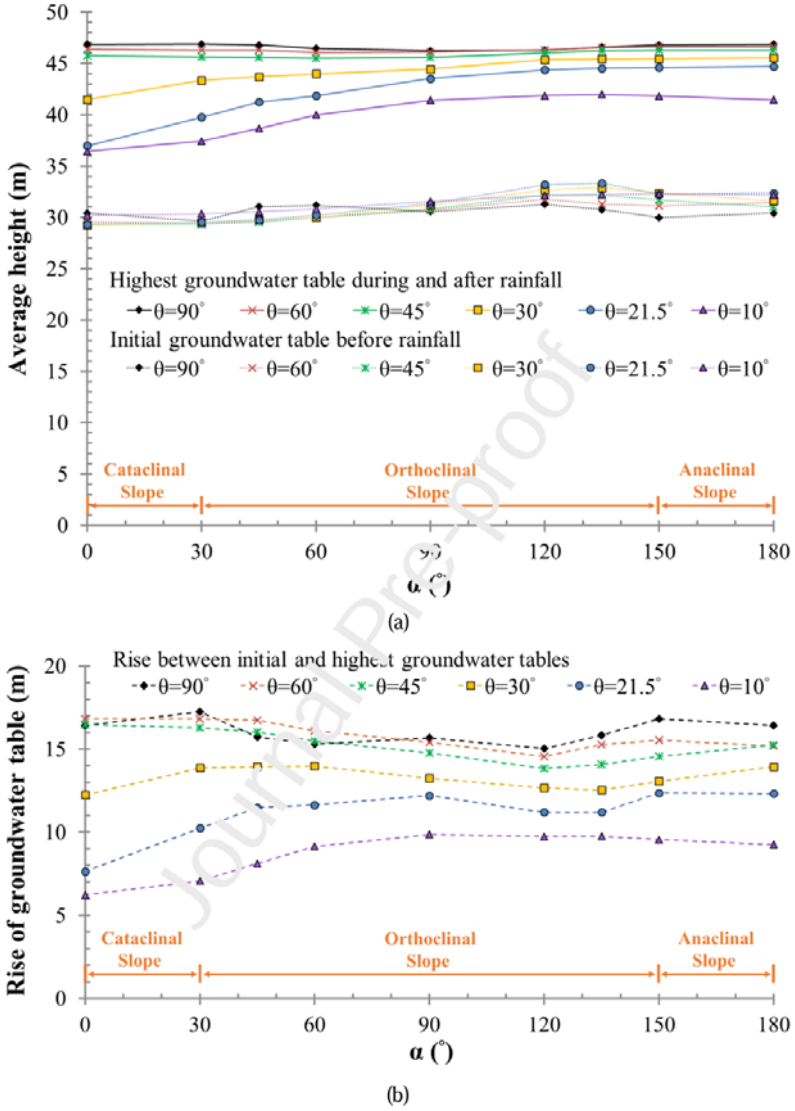

Fig. 14. Average heights of groundwater tables with various dip directions of bedding planes: (a) initial and highest groundwater tables under rainfall and (b) rise of groundwater table.

RESULTS – FACTOR OF SAFETY (FOS)

FOS CHANGES:

- SIGNIFICANT FOS REDUCTION IN STEEP SLOPES (60°) COMPARED TO GENTLE SLOPES (21.5°).
- GRAPH: INITIAL AND FINAL FOS VALUES FOR DIFFERENT BEDDING PLANE ORIENTATIONS.
- CONCLUSION: FOS VARIES WITH BEDDING PLANE ANGLE, WITH LOWEST STABILITY AT STEEP ANGLES DURING HEAVY RAINFALL.

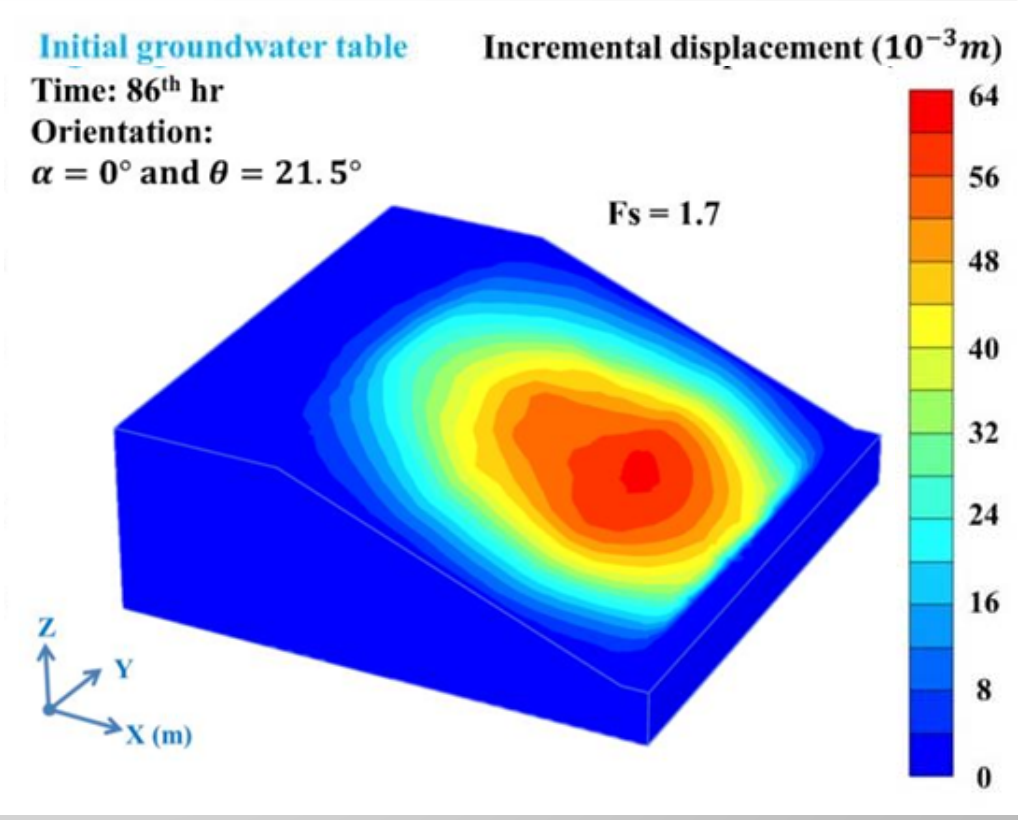

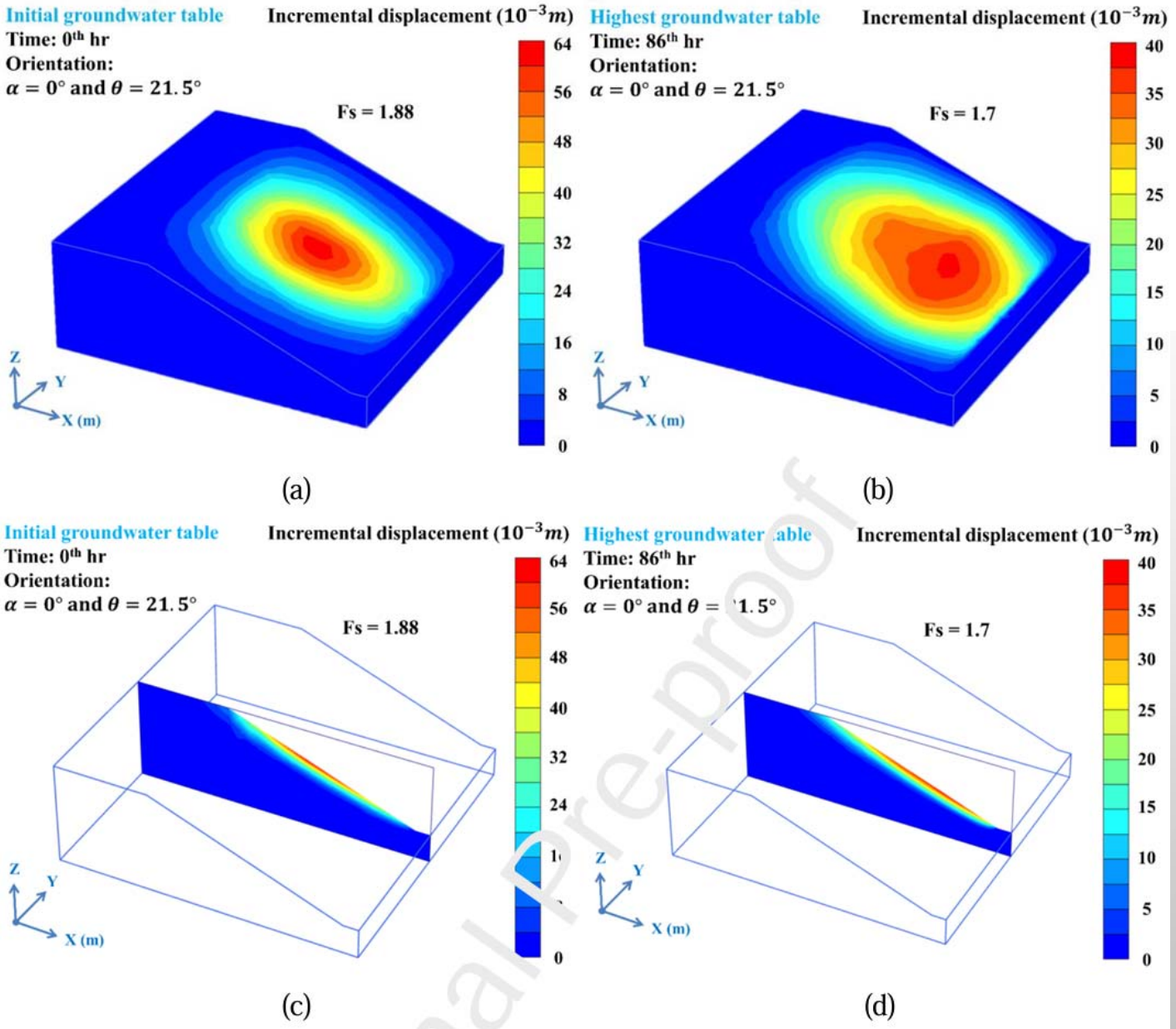

Fig. 15. Factors of safety and potential sliding surfaces of the slope under the initial and highest groundwater table: (a) (b) oblique view and (c) (d) central longitudinal section.

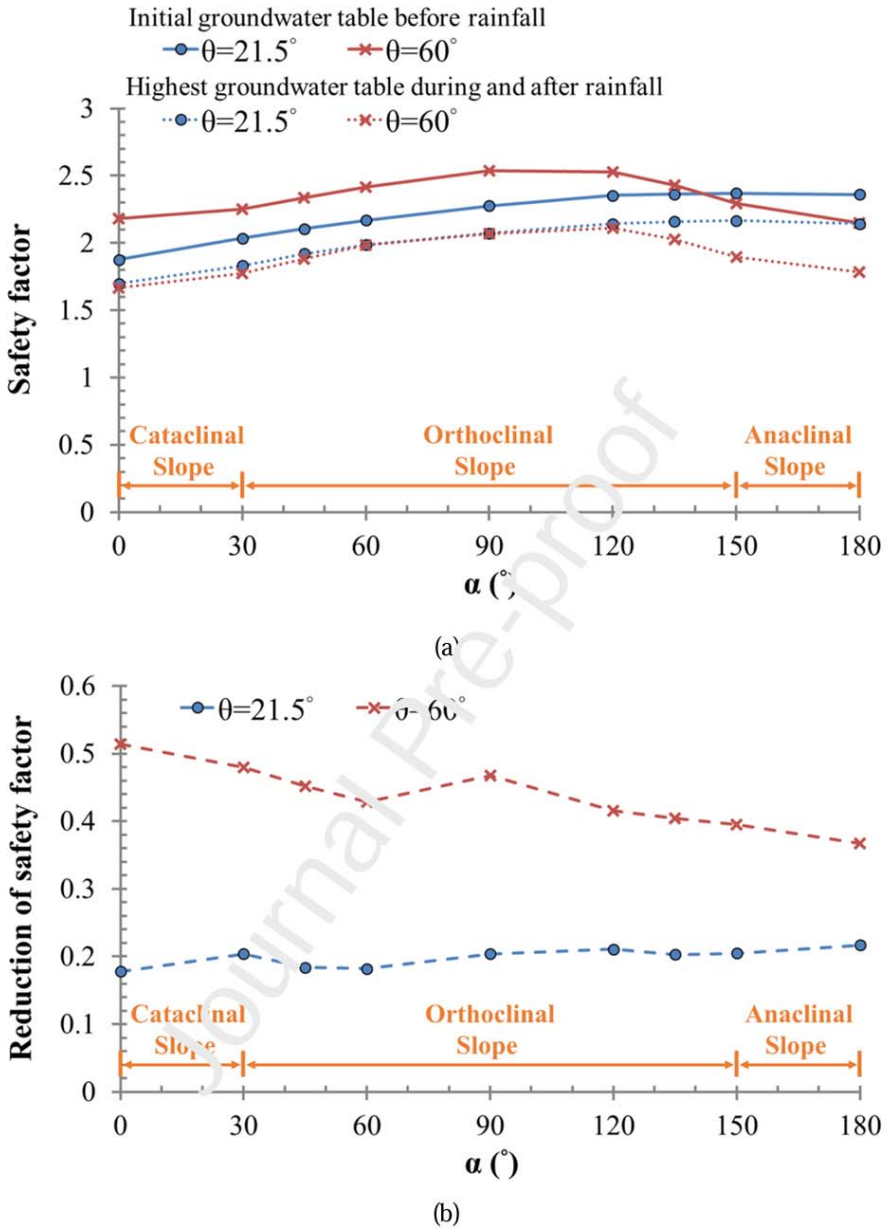

Fig. 16. The factors of safety for various dip directions of bedding planes: (a) initial and highest groundwater tables under rainfall and (b) reduction in the factor of safety due to rainfall.

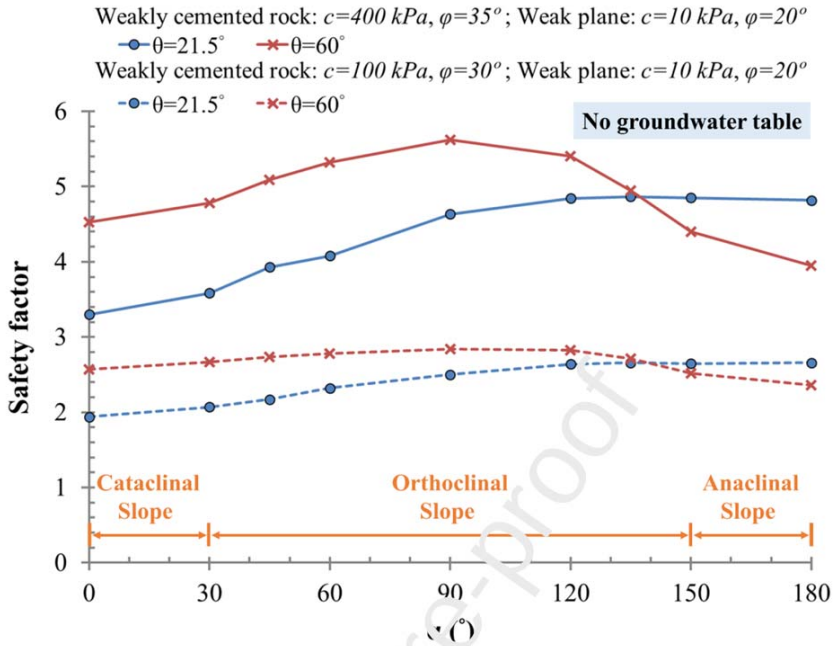

Fig. 17. The factors of safety for various dip directions of bedding planes under dry condition with different strength parameters .

Table 3. Time to reach maximum pressure head, rise of groundwater table, and reduction of safety factor compared among cataclinal, orthoclinal, and anaclinal slopes: (a) gently and (b) steeply dipping bedding planes.

(a)

The dip angle of bedding planes = 21.5°			
	Cataclinal slopes	Orthoclinal slopes	Anaclinal slopes
Time to reach maximum pressure head at a certain position (e.g. Zone 4 at depth of 9~12m)	Longer (3.9~4.3T)*	Moderate (2.5~3.6T)*	Shorter (2.4T)*
Rise of groundwater table	Lower (7.6~10.2m)**	Moderate (11.2~12.2m)**	Higher (12.3~12.4m)
Reduction of safety factor	Smaller (0.18~0.2)***	Moderate (0.18~0.21)***	Larger (0.21~0.22)***

* Refer to Fig. 12(a), and T= 56 hrs, which is the time at peak rainfall intensity

** Refer to Fig. 14(b)

*** Refer to Fig. 16(b)

(b)

The dip angle of bedding planes = 60°			
	Cataclinal slopes	Orthoclinal slopes	Anaclinal slopes
Time to reach maximum pressure head at a certain position (e.g. Zone 4 at depth of 9~12m)	Longer (2.5~2.6T)*	Shorter (1.9~2.2T)*	Longer (2.1~2.5T)*
Rise of groundwater table	Higher (16.8m)**	Moderate (14.6~16.7m)**	Lower (15.2~15.5m)**
Reduction of safety factor	Larger (0.48~0.51)***	Moderate (0.4~0.47)***	Smaller (0.37~0.4)***

* Refer to Fig. 12(b), and T= 36 hrs, which is the time at peak rainfall intensity

** Refer to Fig. 14(b)

*** Refer to Fig. 16(b)

IDENTIFIED UNFAVORABLE CONDITIONS

FOUR KEY CONDITIONS:

- 1. DAYLIGHT CONDITION (BEDDING PLANES DIPPING OUT OF THE SLOPE).
- 2. COINCIDING BEDDING PLANES AND SLOPE FACE.
- 3. STEEPLY DIPPING PLANES OUTWARDS.
- 4. STEEPLY DIPPING PLANES INWARDS.

IMPACT:

THESE CONDITIONS EXACERBATE INSTABILITY, NEEDING CAREFUL ATTENTION IN SLOPE DESIGN.

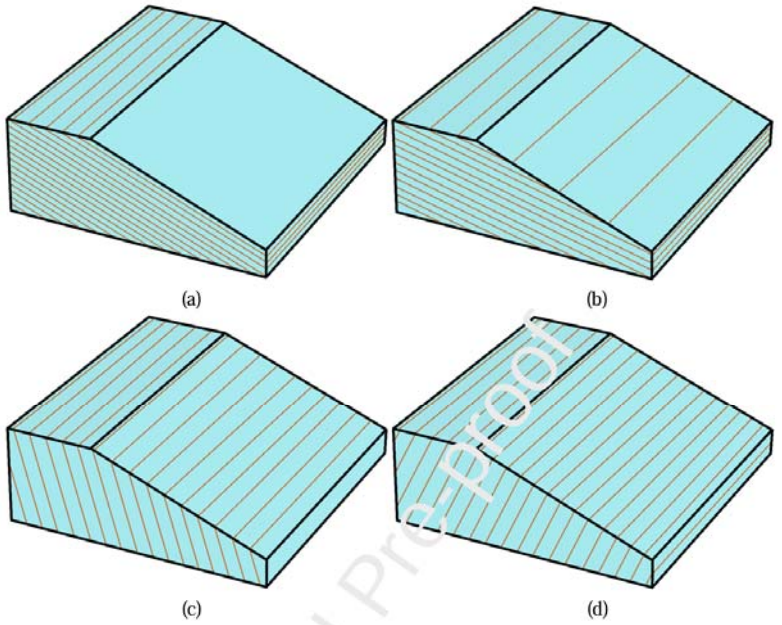

Fig. 18. The unfavorable bedding plane-slope conditions for slope stability where the bedding planes and the slope face approximately strike in the same direction: (a) the coinciding condition of bedding planes and the slope face, (b) the daylight condition of bedding planes, (c) steep bedding planes that dip out the slope, and (d) steep bedding planes that dip into the slope.

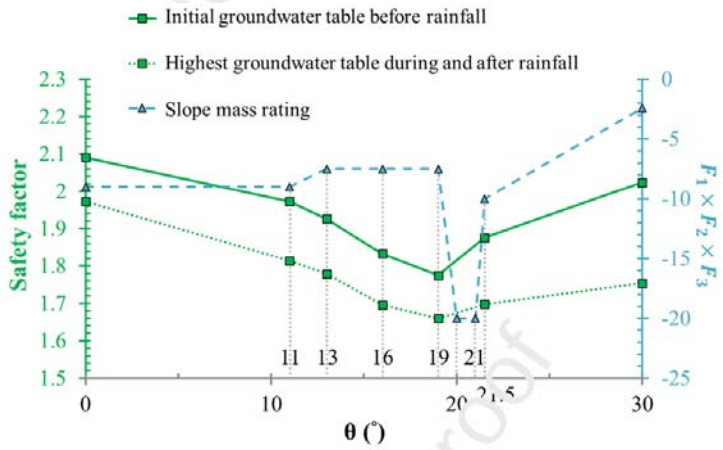

Fig. 19. Variations of safety factor and slope mass rating with the dip angle of bedding planes under the daylight condition (The slope face and the bedding planes dip in the same direction (α=0°), and θ of 21.5° represents the coinciding condition).

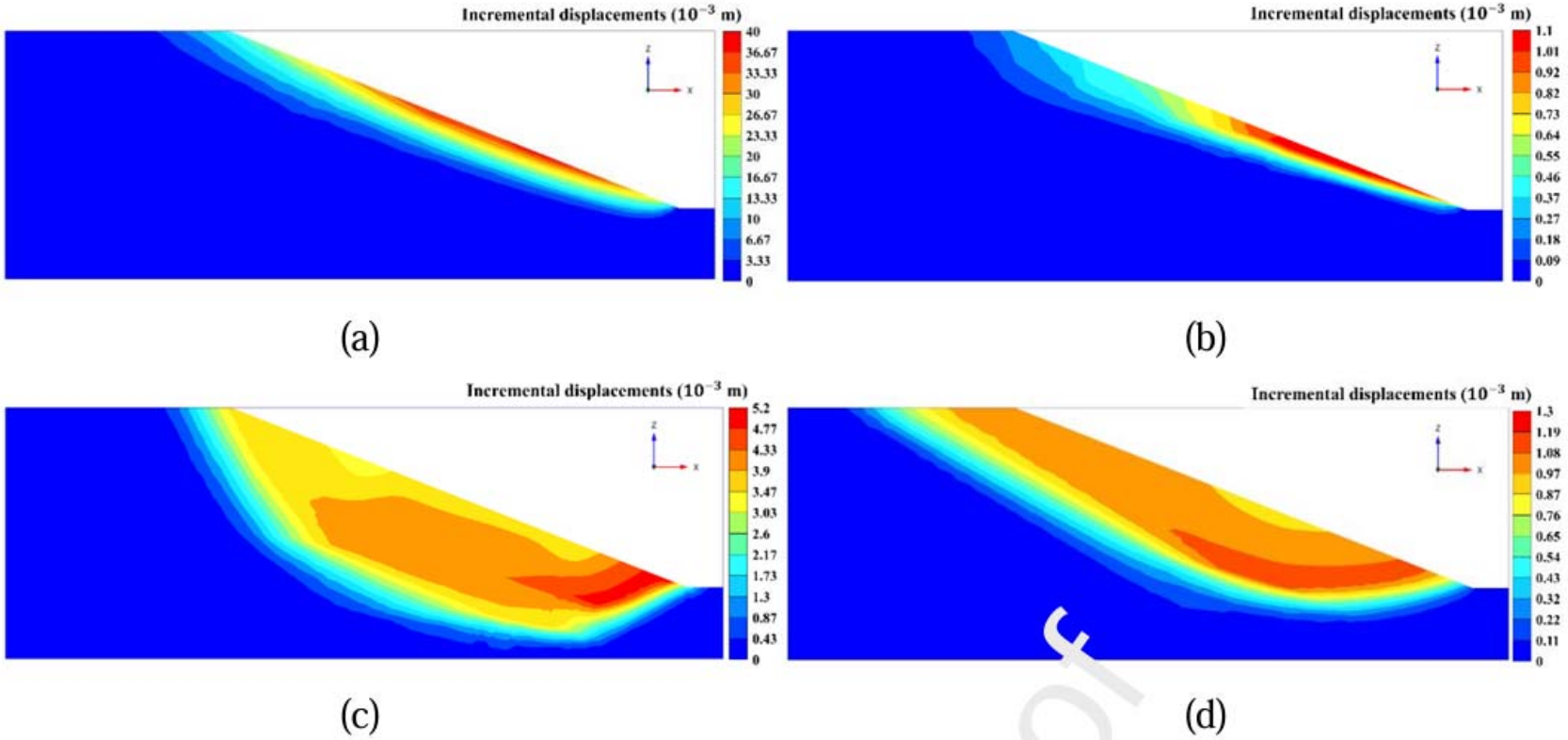

Fig. 20. The cross-sections of the failure surfaces that correspond to the unfavorable conditions in Fig. 18: (a) the coinciding condition of bedding planes and the slope face, (b) the daylight condition of bedding planes, (c) steep bedding planes that dip out the slope, and (d) steep bedding planes that dip into the slope.

DISCUSSION

ANISOTROPY IMPLICATIONS:

- BOTH PERMEABILITY AND STRENGTH ANISOTROPY CRITICAL TO SLOPE STABILITY.
- 3D MODELING REVEALS DETAILED FAILURE MECHANISMS THAT 2D MODELING CANNOT CAPTURE.

REAL-WORLD RELEVANCE:

- FINDINGS ARE APPLICABLE IN MOUNTAINOUS REGIONS WITH STRATIFIED ROCKS, ESPECIALLY IN RAINFALL-PRONE AREAS.

FUTURE WORK

EXTENSIONS:

- INCLUDE UNSATURATED FLOW MODELS FOR MORE REALISTIC SIMULATIONS.
- ANALYZE DIFFERENT RAINFALL INTENSITIES AND DURATIONS.

APPLICATION:

- POTENTIAL TO DEVELOP PREDICTIVE MODELS FOR LANDSLIDE SUSCEPTIBILITY UNDER VARIOUS GEOLOGIC SETTINGS.

CONCLUSION

SUMMARY:

- 3D SIMULATIONS ILLUSTRATE THE SIGNIFICANT ROLE OF ANISOTROPY IN SLOPE STABILITY.
- CRITICAL FINDINGS: STEEP BEDDING PLANES POSE HIGHER RISKS DURING RAINFALL.
- RECOMMENDATIONS FOR FIELD ASSESSMENTS IN STRATIFIED, RAINFALL-PRONE REGIONS.

國立中央大學
National Central University

THANK YOU FOR LISTENING

- OPEN FLOOR FOR AUDIENCE QUESTIONS.